Eur Biophys J (1984) 11:35–42

European Biophysics Journal

Impurity controlled phase transitions of phospholipid monolayers

M. Lösche and H. Möhwald

Technische Universität München, Physik-Department, E 22 (Biophysik), D-8046 Garching, Federal Republic of Germany

Received March 27, 1984/Accepted May 10, 1984

Abstract. The phase diagram of monolayers of L-α-dimyristoyl phosphatidic acid has been studied by fluorescence microscopy. For pressures corresponding to the nearly horizontal slope in the pressure area diagram the growth of crystalline platelets can be observed. They are of dendritic nature; their sizes can be controlled via pressure, compression speed, temperature and pH, and increased up to 100 μm. Due to repulsive interaction a hexagonal arrangement of crystalline platelets can be established.

It is shown that the textures do not depend on the dye probe for concentrations below 3 mol%. On the other hand via incorporation of impurities in concentrations of about 1 mol% the coexistence of lipid and solid phases can be controlled. Since, for a constant surface pressure, this coexistence can be maintained, these monolayers are suitable model systems to study the interactions of proteins and vesicles with coexisting fluid and solid membrane areas.

Key words: Interfaces, phospholipid monolayers, phase transitions, fluorescence microscopy

Introduction

Lipid monolayers are suitable model systems for studying the interactions in biological membranes (Phillips 1972). They allow the variation of many independent parameters, but only a few techniques are suitable for their characterization. Therefore there is still confusion as regards the phase diagram of the best-investigated phospholipid, L-α-dipalmitoylphosphatidylcholine (DPPC). Whereas the horizontal slope in the pressure area diagram was ascribed to a transition from a liquid expanded to a liquid condensed state (Cadenhead et al. 1980) or from a liquid to a solid (Albrecht et al. 1978) state, respectively, v. Tscharner and McConnell (1981) claimed that this region corresponded to a homogeneous phase. Although the latter conclusion was wrong (see Lösche et al. 1983; Peters and Beck 1983) the technique they applied, fluorescence microscopy, has proved to contribute significantly to an understanding of monolayers. It yields a high contrast and, using suitable dyes, is sensitive to environmental parameters. However, the interpretation of results depends on an understanding of the behaviour of the probe and of possible distortions of the system due to the incorporation of probes.

To assess the influence of the probe we increased the sensitivity of our fluorescence microscopic set-up so that we could work with probe concentrations as low as 0.1 mol% and studied surface textures for various compositions. By this, we demonstrate that phase transitions can be studied and that the features observed are those of the pure lipid. In addition, we show that the crystallization can be controlled via the impurity induced melting point reduction. Using Raoult's law, the influence of impurities on the increase in the slope of the isotherm is estimated to be about the same order as calculated in Monte Carlo calculations by Georgallas and Pink (1981).

Experimental

The fluorescence microscope has been described in detail by Lösche and Möhwald (1984). A water immersion objective is inserted into the bottom of a film balance. Fluorescence excitation is achieved via a 450-W Xe lamp, suitable filters and a dichroic mirror. Surface textures can be observed by a SIT video camera and photographed from a TV screen. The lateral resulution of the optical set up is better than

Abbreviations: DMPA, L-α-dimyristoyl phosphatidic acid; DPPC, L-α-dipalmitoylphosphatidylchline; DP-NBD-PE, L-α-dipalmitoyl-nitrobenzoxadiazol-phosphatidylethanolamin; diO-C_{18} (3), 3,3′-dioctadecyl-oxocarbocyanin

2 μm; the accuracy of pressure measurements is better than 0.1 mN/m. Of special importance is the stability of the system, allowing measurement times of more than 6 h.

The phospholipid L-α-dimyristoyl phosphatidic acid (DMPA) studied was purchased from Fluka (Buchs, Switzerland) and checked chromatographically for purity. The dye probe L-α-dipalmitoyl-nitrobenzoxadiazol-phosphatidylethanolamine (DP-NBD-PE) was purchased from Avanti Biochem.; the dye 3,3′-dioctadecyloxocarbocyanin [diO-C_{18}(3)] was prepared by Dr. Wirthensohn in our laboratory. The phospholipid/dye mixture was spread from a 3 : 1 chloroform/methanol solution. The water used was distilled and filtered (pH 5.6). For measurements at pH = 8 (Fig. 4) phosphate buffer was used.

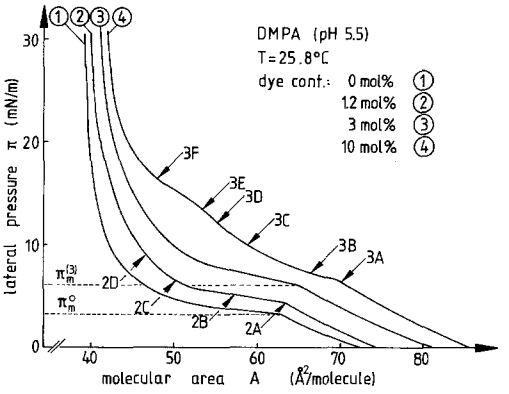

Fig. 1. Surface pressure versus area diagram of L-α-dimyristoyl phosphatidic acid; pH = 5.5, T = 25.8° C. The concentration of the dye DP-NBD-PE amounts to 0 mol% (curve 1), 1.2 mol% (curve 2), 3 mol% (curve 3), and 10 mol% (curve 4). Arrows and letters denote positions in the diagram where micrographs in Figs. 2 and 3 were taken

Results

Figure 1 shows pressure/area diagrams for monolayers of DMPA containing the dye DP-NBD-PE in concentrations between 0 and 10 mol%. The change in the slope of the pressure area diagram, corresponding to the liquid/solid transitions, is clearly observed at an area per molecule around 65Å^2. The corresponding pressure increases from 3.5 mN/m for "pure" DMPA to 6.5 mN/m for a dye content of 3 mol% [curve (3)]. This increase occurs about linearly with dye concentration within these concentration limits. For a higher dye content (e.g., 10 mol%) the transition pressure is about constant. Instead, a second transition is observed at a pressure of about 15 mN/m.

Typical surface textures for low dye concentration (0.2–3 mol%) and for high dye concentrations (10 mol%) are given in Figs. 2 and 3 as a function of pressure. Whereas at pressures below the one corresponding to the liquid/solid phase transition, π_m (see Fig. 1), a homogeneous monolayer is observed, above that point dark spots appear. These spots, when observed, already have diameters of some micrometres. Although the lateral resolution of our apparatus (2 μm) is sufficient, we do not observe the growth of the dark areas up to the size given in Fig. 2A. This indicates, but does not yet prove, that the dark spots correspond to crystalline nuclei. Further increase of the pressure enlarges the dark areas. We discuss the physics of the observed textures more quantitatively in the Discussion.

The dark surface corresponds to crystalline areas that hardly dissolve the dye and hence do not fluoresce. The crystals exhibit dendritic growth on further increasing the pressure (Fig. 2B). At a high enough pressure an almost completely crystallized surface results (Figs. 2C, D). The dye is squeezed out into the remaining liquid domains. These domains gradually disappear with time constants in the order of hours. This may be due to a condensation of the dye in dye-enriched regions that do not fluoresce as they exhibit self-quenching.

The size of the dendrites can be varied with compression speed, the largest sizes of the order of 100 μm appearing with the minimum compression rate of 0.2 Å^2/molecule/min.

The textures observed at a high dye content (10 mol%, Fig. 3) are similar to those observed at low concentrations only for pressures between 6.6 and 15 mN/m (Figs. 3A–C). However, a gradient of dye concentration is observed from the gradient of brightness within the crystalline areas of Fig. 3C and more clearly in the subsequent Figs. 3D–F. At higher pressures, corresponding to the second change in the slope of the pressure/area diagram [Fig. 1, curve (4)], a darker ring appears at the border lines of the dendrites (Fig. 3D). On further increasing the pressure the newly created areas increase in size. Finally, at a very high pressure the crystallites cover the surface almost completely and between different dendrites only small bright areas remain. The crystalline spots exhibit two distinctly different zones. The bright centre is hemmed by a dark edge with a size of several micrometers. In addition the crystalline areas are of about the same size and arranged in hexagonal order.

Figure 4 demonstrates more clearly that at different conditions of preparation (pH ≥ 8) crystallites can be formed which at a sufficiently high pressure are arranged in a hexagonal pattern. These patterns form during the process of crystallization while different crystallites still exhibit distances of more

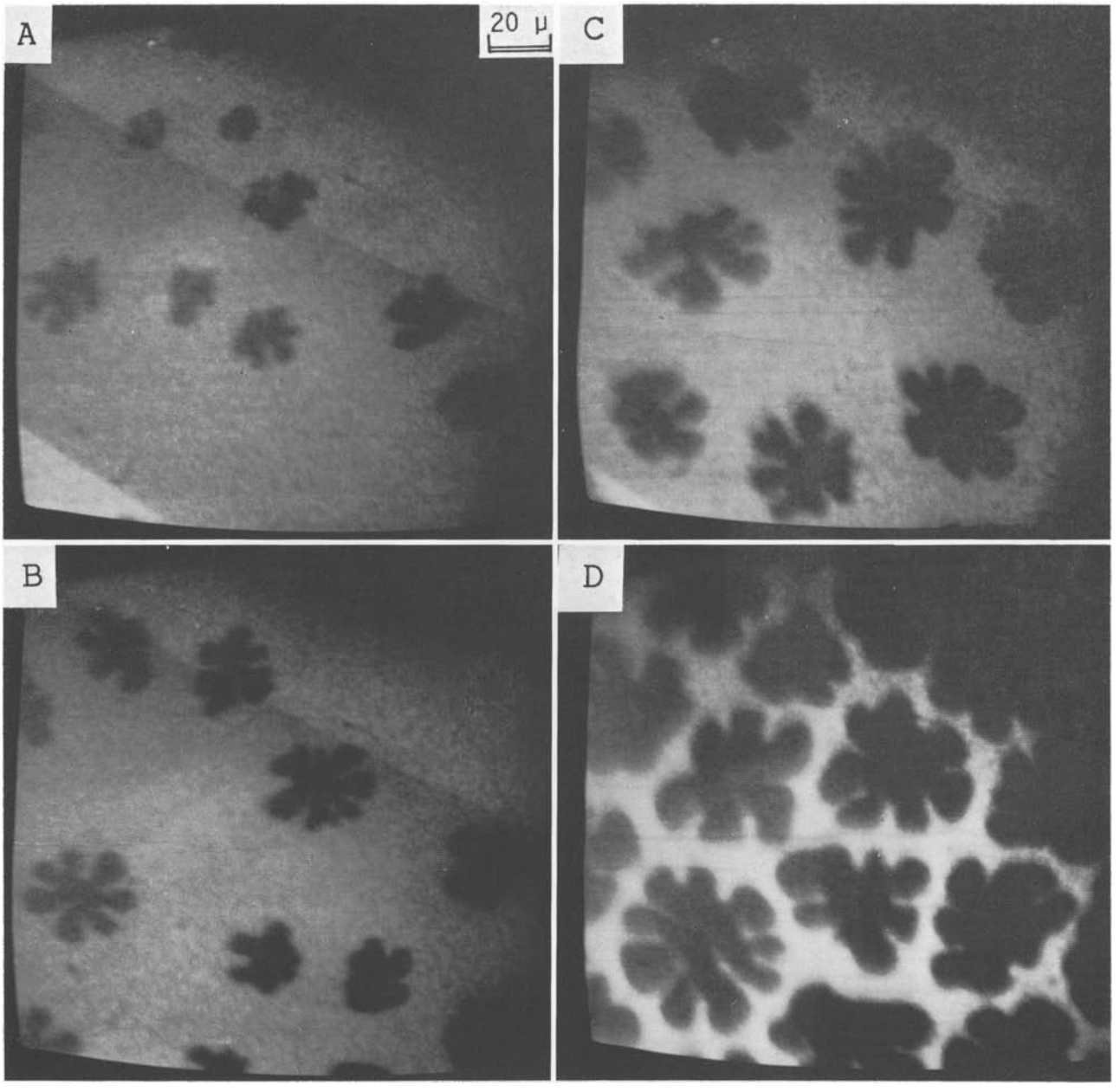

Fig. 2. Fluorescence micrographs of a DMPA monolayer containing 1.5 mol% of the dye DP-NBD-PE. The corresponding surface pressures, increasing from A to D are given in Fig. 1 (T = 25.5° C, pH 5.5)

than 20 µm. There apparently exist long-range repulsive forces, probably electrostatic ones, which will be discussed in another publication (Fischer et al. 1984). We will then also discuss dipolar forces that may be responsible for the uniform size and shape of the crystalline areas on the water surface.

Using another probe, the cyanine dye diO-C_{18} (3), the textures are similar to those observed with DP-NBD-PE. Especially also with this dye basically the same geometries appear, namely "clover leaves" and "coffee beans". At high concentrations of 10 mol% we observed even nuclei as starting points for crystal growth. Figure 5 shows these to be bright centres of the crystallites, i.e., dye-enriched areas.

Discussion

General aspects

The present study on the liquid/solid phase transition of a phospholipid by a new technique not only facilitates the understanding of lipid monolayers as

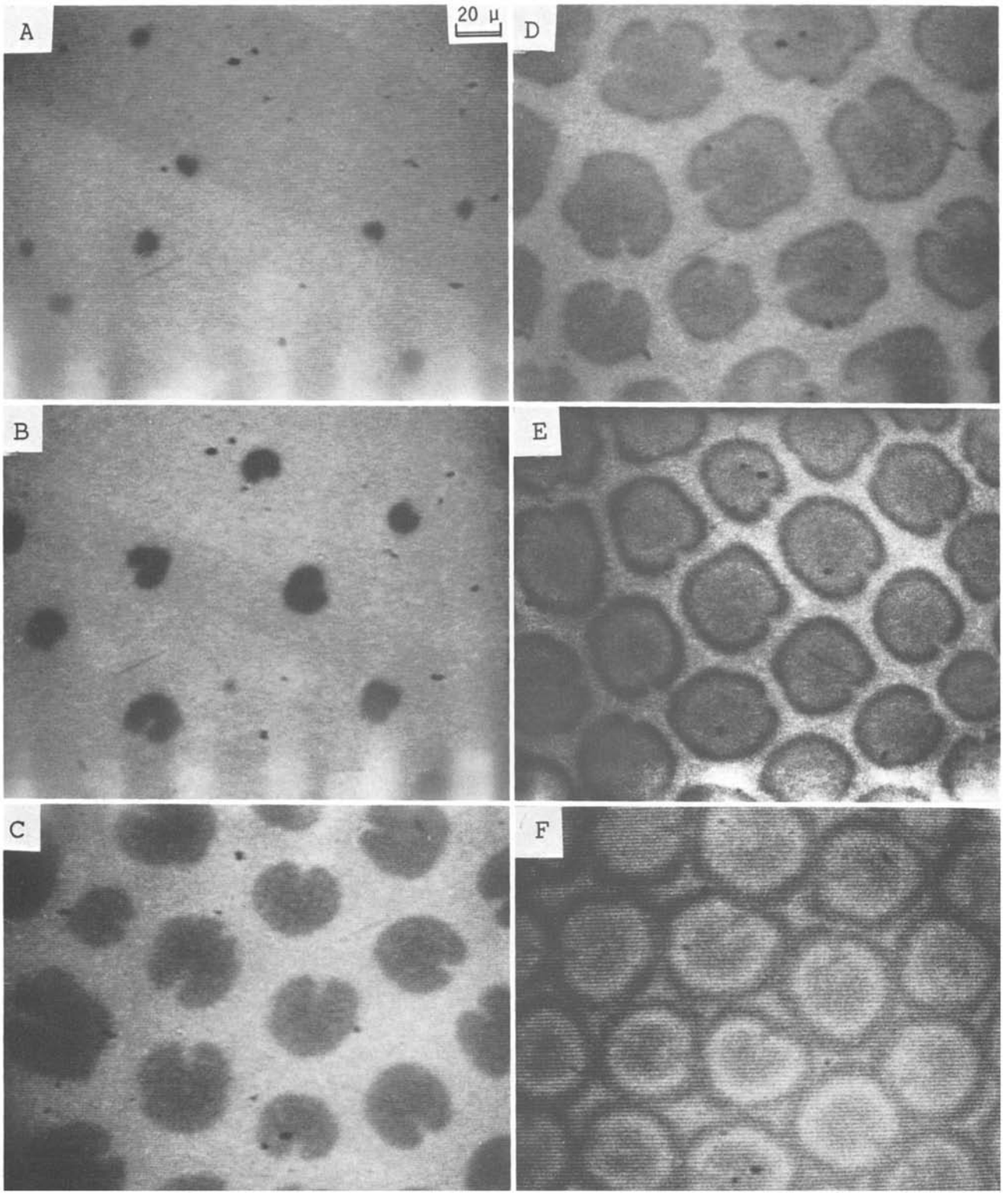

Fig. 3. Fluorescence micrographs of a DMPA monolayer containing 10 mol% of the dye DP-NBD-PE. The corresponding surface pressures are given in Fig. 1 (T = 25° C, pH 5.5). The photographs taken at higher pressures (Fig. 3E, F) were developed for higher contrast compared to Fig. 3A–D

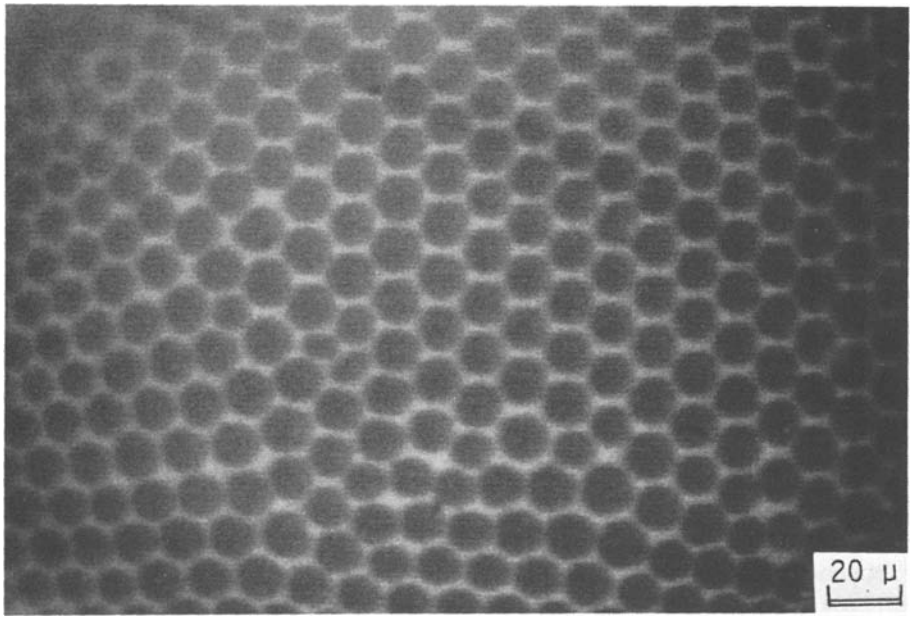

Fig. 4. Fluorescence micrograph of a DMPA monolayer containing 0.3 mol% of the dye DP-NBD-PE; pH 8, T = 18° C, π = 40 mN/m

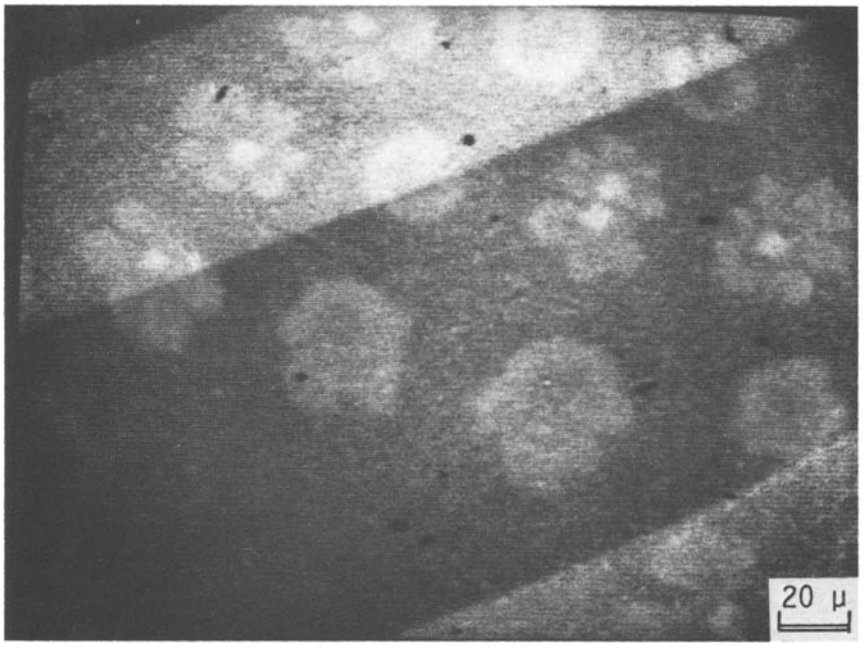

Fig. 5. Fluorescence micrograph of a DMPA monolayer containing 10 mol% of the dye diO-C_{18} (3); pH 5.5, T = 26° C, π = 20 mN/m

biophysical model systems, it also opens perspectives to study microscopically the interactions of molecules (e.g., proteins) in the subphase with a model membrane. In these studies, a special benefit will result from the fact that over a wide pressure range a coexistence between liquid and solid surface can be established and controlled. The discussion shall therefore concentrate on this coexistence and quantitatively consider a model to explain the coexistence. Before developing that model we will prove three statements: (*1*) The areas appearing dark at low dye concentrations, and with convex boundary are crystalline.

The clearest proof of this results from electron diffraction measurements of these monolayers transferred on suitable supports (Lösche et al. 1984; Fischer and Sackmann 1984). Hexagonal diffraction patterns characteristic of long-range crystalline order are observed within these areas.

(*2*) The two dyes used are insoluble in the crystalline lipid domains.

This immediately follows from the observation of the low fluorescence intensity of the crystallites at low dye concentration. In accordance with this, as the dye is enriched in the remaining liquid domains during crystallization, local dye concentrations above 20 mol% are expected. In this case a self-quenching of the dye has to be expected, leading to reduced fluorescence (Lösche et al. 1983). In addition a phase segregation into an extremely dye rich (dark) and a less concentrated (bright) domain can occur. This is indeed observed as a segregation into the dark hem formed at a pressure above 15 mN/m (Fig. 3D) and into the residual bright areas.

In addition, it might be surprising that the dye DP-NBD-PE which, due to the long palmitoyl chains, forms a solid monolayer at pressures above 3 mN/m (data not shown), is insoluble in the solid phase of the lipid DMPA. This may be a peculiar feature of this phospholipid as the crystalline phase is extremely condensed compared to phospholipids like DPPC, exhibiting also a bulky head group.

(*3*) The shapes of the crystallites are not influenced by the dye used.

There is a variety of shapes of crystallites, which can basically be classified as "clover leaves" and "coffee beans", with sizes controllable by compression speed. In addition, the border lines between dendrites of one crystalline patch can be annealed. However, these structures do not depend on dye concentration (0.25 mol%–10 mol%), do not vary for two different dyes used and are even observed electron microscopically without using any dye or staining material (Lösche et al. 1984). Hence the structures formed are not characteristic of the dye. However, one may conclude from the discussion below that by incorporation of impurities being soluble preferentially in the solid phase a different surface texture is expected.

Impurity control of crystallization

Although we have demonstrated above that the surface textures do not depend on the dye used, we will show subsequently that the crystallization process can be controlled by impurities. The ideas, sketched for a one-dimensional process in Fig. 6, are the following:

(*1*) The liquid/solid transition is a first-order phase transition, the finite slope in the pressure area diagram being due to impurities, as explained below.

(*2*) On increasing the pressure to a value π_1 larger than π_m, nuclei as centres for crystal growth are formed.

(*3*) Having a size larger than a critical value these nuclei grow to form two-dimensional crystals. As the images in Figs. 2 and 3 indicate, during a change in pressure the size of the crystals increases, but their numbers do not.

(*4*) Not being soluble in the solid phase, impurities are squeezed out into the liquid phase.

(*5*) The increase in impurity content of the liquid phase leads to a melting point reduction or, according to Raoult's law, to an increase in the equilibrium pressure π_{eq} for crystallization. In thermodynamic equilibrium the experimentally applied pressure is equal to π_{eq} at the solid/liquid boundary.

(*6*) On further increasing the pressure (e.g., to π_2, Fig. 6) crystallization proceeds and π_{eq} is increased until the new equilibrium is established.

Thus at a defined pressure and temperature the crystallization process can be controlled. In particular, the ratio of liquid and crystalline surface areas can be varied via the pressure or maintained constant. This is possible at least over periods of hours, as we were able to observe in our fluorescence microscopy experiment. This model also explains why we observe dendritic growth which is typical for a supercooled melt (Chalmers 1964). The interaction between dendrites occurs either via transfer of (latent) heat or, most probably, of impurities out of crystallized areas. Heat or foreign molecules accumulate in the liquid area between the dendrites, thereby retarding crystallization in this area. Thus zones of high impurity content remain between two dendrites, as is observed in Fig. 2D. When there is two-dimensional crystal growth accumulation of heat is not very probable, as there will be an efficient heat transfer into the water subphase. Surface active impurities, however, remain in the monolayer and may accumulate at least during the initial nucleation period. Thus this type of growth, "constitutional supercooling", may occur.

At this point we have to point out that, although during the short initial growth period the impurity distribution may be inhomogeneous in the liquid phase, this does not hold during the observation period for our experimental compression speeds. As is observed for the dye, impurities squeezed out of the solid phase are quickly distributed throughout the liquid. This can be estimated as follows.

For the simplest case of a one-dimensional system the impurity concentration in the liquid phase, c_{Imp} as a function of distance x from the solid/liquid interface is given according to (Chalmers 1964, pp 132–136)

$$c_{Imp} = c_0 * \left[1 + \frac{1-k}{k} * \exp\left(-\frac{v}{D} x \right) \right], \qquad (1)$$

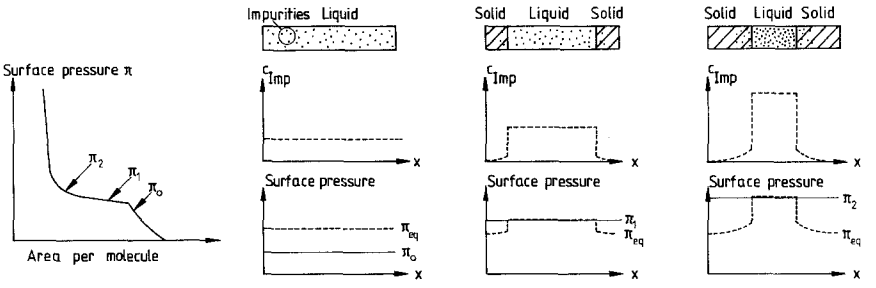

Fig. 6. Sketch of the impurity distribution c_{Imp} and the equilibrium melting pressure π_{eq} for various states during the solidification

where c_0 is the concentration for $x \to \infty$ and the partition coefficient between the solid and liquid phase, k, may be assumed to be much smaller than 1. The diffusion coefficient D is of the order of 10^{-7} cm^2/s (Peters and Beck 1983). In the experiments we observe growth velocities v for solid surfaces below 10^{-5} cm/s.

Hence $v/D \simeq 100\ cm^{-1}$, i.e., at distances below 20 μm between the dendrites the impurity distribution is homogeneous. This also means that at any point in the liquid phase the melting point reduction due to impurities is uniform.

On the other hand one expects an inhomogeneous dye distribution in the solid phase, as is sketched in Fig. 6. This is due to the fact that during crystallization the dye content in the liquid phase is increased and the ratio of dye concentrations at the interface of the two phases is determined by the partition coefficient. Due to the low diffusion coefficient in the solid phase this gradient is frozen in and can be observed at high dye concentrations (cf. Fig. 3).

Finally we want to show quantitatively that impurity concentrations of about 2 mol% can be sufficient to control the crystallization process. For this we use, as an easily observable impurity, the dye that is dissolved mainly in the liquid phase.

Raoult's law describes the increase in transition pressure $\Delta\pi_{eq}$ as a function of impurity concentration c_{Imp} (Albrecht et al.1981):

$$\Delta\pi_{eq} = \frac{k_B T}{\Delta A} * c_{Imp} \,. \tag{2}$$

As we cannot determine the difference ΔA in molecular area of the dye between solid and liquid phase, we determine the coefficient in Eq. (2) experimentally. This is done by measuring the pressure π_m corresponding to the onset of the phase transition as a function of dye content. One obtains

$$\frac{\Delta\pi_{eq}}{c_{Imp}} \simeq 1\ \mathrm{Mn/m}\ \ (c_{Imp}\ \text{in mol\%}) \tag{3}$$

Table 1

c_{Dye} [mol%]	$\pi_{1/2} - \pi_c$ [mN/m]	$c_{Imp} = c_{Dye} + c_?$ [mol%]	$c_?$ [mol%]
0.3	2	2	1.7
1.5	3.3	3.3	1.8

as can be estimated from Fig. 1, which for the purpose of clarity contains only a few of our data. This result is about a factor of 2 larger than the value observed by Albrecht et al. (1978) for cholesterol in phospholipids and calculated by Georgallas and Pinck (1981).

From a comparison of fluorescence micrographs and pressure area diagrams we can also determine the pressure $\pi_{1/2}$ corresponding to half completion of the phase transition. At this pressure the dye content of the liquid phase is increased by a factor of 2. Table 1 gives the pressure increase during the transition for two dye concentrations. With Eq. (3) we can thus calculate the impurity content, c_{Imp}, of the monolayer that is the sum of dye content, c_{Dye}, and an unknown impurity, $c_?$.

The experiments with the different dye concentrations consistently show agreement in the determined value $c_?$. This demonstrates that the solidification of the monolayer can be controlled by impurities in concentrations around 1 mol%. On the other hand, although the value given for an unknown material is not unrealistic, it does not prove its existence. We basically calculated that at low dye content the pressure-area diagram and the solidification are not influenced by the dye and that there are other contributions to the finite slope in the diagram. This may be other impurities, but it may also be electrostatic forces, as discussed by Fischer et al. (1984b).

Concluding remark

We have shown then that although impurities do not necessarily change the phase behaviour of a monolayer, they may be used to control the solid/liquid

transition. This offers the possibility of maintaining coexistence between different phases in order to study microscopically the interaction of proteins and vesicles with various states of a membrane.

Acknowledgement. Helpful discussions with E. Sackmann are gratefully acknowledged. This work was supported by the Deutsche Forschungsgemeinschaft (Mo 283/9).

References

Albrecht O, Gruler H, Sackmann E (1978) Polymorphism of phospholipid monolayers. J Phys (Paris) 39: 301–313

Albrecht O, Gruler H, Sackmann E (1981) Pressure-composition phase diagrams of cholesterol/lecithin, cholesterol/phosphatidic acid, and lecithin/phosphatidic acid mixed monolayers: a langmuir film balance study. J Colloid Interface Sci 79: 319–338

Cadenhead DA, Müller-Landau F, Kellner BMJ (1980) Phase transitions in insoluble one and two-component films at the air/water interface. In: Ordering in two dimensions. Elsevier Biomed. Press, Amsterdam, pp 73–81

Chalmers B (1964) Principals of solidification. Wiley & Sons, New York London Sydney

Fischer A, Sackmann E (1984) Electron microscopy and diffraction study of phospholipid monolayers transferred from water to solid substrate. J Phys (Paris) 45: 517–527

Fischer A, Lösche M, Möhwald H, Sackmann E (1984) On the Nature of the Lipid Monolayer Phase Transition. J Phys (Paris) Lett (in press)

Georgallas A, Pink DA (1981) Phase transition in monolayers of saturated lipids. J Colloid Interface Sci 89: 107–116

Lösche M, Möhwald H (1984) A fluorescence microscope to observe dynamical processes in monomolecular layers at the air/water interface. Rev Sci Instrum (in press)

Lösche M, Sackmann E, Möhwald H (1983) A fluorescence microscopic study concerning the phase diagram of phospholipids. Ber Bunsenges Phys Chem 87: 848–852

Lösche M, Rabe J, Fischer A, Rucha BU, Knoll W, Möhwald H (1984) Microscopically controlled preparation of langmuir-blodgett films. Thin Solid Films (in press)

Peters R, Beck K (1983) Translational diffusion in phospholipid monolayers measured by fluorescence microphotolysis. Proc Natl Acad Sci USA 80: 7183–7187

Phillips MC (1972) The physical state of phospholipids and cholesterol in monolayers, bilayers and membranes. Prog Surf Membr Sci 5: 139–221

Tscharner V v, McConnell HM (1981) An alternative view of phospholipid phase behavior at the air/water interface. Biophys J 36: 409–419